

Generation of tuneable 589nm radiation as a Na guide star source using an optical parametric amplifier

Malte Duering², Vesselin Kolev¹, and Barry Luther-Davies¹

¹Laser Physics Centre, Research School of Physical Sciences and Engineering, The Australian National University, Canberra, ACT 0200

²Fraunhofer-Institut für Lasertechnik ILT, Steinbachstr. 15, 52074 Aachen, Germany
mwd111@rsphysse.anu.edu.au

Abstract: We describe a 5.5W 589nm source based on a passively mode-locked Nd:YVO₄ laser and a multi-stage Lithium Triborate optical parametric amplifier seeded by a tuneable semiconductor laser. We show this system can produce rapidly tuneable, transform-limited pulses in near diffraction-limited beams at 589nm, useful for Na guide star applications. The attraction of this scheme is that it can be assembled from commercially available hardware and is readily scalable to high average powers.

©2009 Optical Society of America

OCIS codes: (190.4410) Nonlinear optics, parametric processes.

References and links

1. H. W. Babcock, "The possibility of compensating astronomical seeing," *Publ. Astron. Soc. Pac.* **65**, 229-236 (1953).
2. N. Ageorges and C. Dainty, *Laser Guide Star Adaptive Optics for Astronomy* (Kluwer Academic Publishers, 2000).
3. A. Tracy, A. Hankla, C. Lopez, D. Sadighi, N. Rogers, K. Groff, I. McKinnie and C. d'Orgeville, "High-Power Solid-State Sodium Beacon Laser Guidestar for the Gemini North Observatory," *Proc. SPIE* **5490**, 998-1009 (2004).
4. C. E. Max, K. Avicola, J. M. Brase, H. W. Friedman, H. D. Bissinger, J. Duff, D. T. Gavel, J. A. Horton, R. Kiefer, J. R. Morris, S. S. Olivier, R. W. Presta, D. A. Rapp, J. T. Salmon and K. E. Waltjen, "Design, layout, and early results of a feasibility experiment for sodium-layer laser-guide-star adaptive optics," *J. Opt. Soc. Am. A.* **11**, 813-824 (1994).
5. T. H. Jeys, A. A. Brailove and A. Mooradian, "Sum frequency generation of sodium resonance radiation," *Appl. Opt.* **28**, 2588-2591 (1989).
6. N. Saito, K. Akagawa, Y. Hayano, Y. Saito, H. Takami, M. Iye, S. Wada, "Synchronization of 1064 and 1319 nm pulses emitted from actively mode-locked Nd : YAG lasers and its application to 589 nm sum-frequency generation," *Jpn. J. Appl. Phys. Part 2* **44**, L1484-L1487 (2005).
7. C. A. Denman, P. D. Hillman, G. T. Moore, J. M. Telle, J. D. Drummond, and A. L. Tuffli, "20 W CW 589 nm sodium beacon excitation source for adaptive optical telescope applications," *Opt. Mater.* **26**, 507-513 (2004).
8. A. Tracy, A. Hankla, C. Lopez, D. Sadighi, N. Rogers, K. Groff, I. McKinnie, and C. d'Orgeville, "High-Power Solid-State Sodium Beacon Laser Guidestar for the Gemini North Observatory," *Proc. SPIE* **5490**, 998-1009 (2004).
9. J. Bienfang, et al., "20W of continuous-wave sodium D2 resonance radiation from sum-frequency generation with injection-locked lasers," *Opt. Lett.* **28**, 2219-2221 (2003).
10. N. Saito, et al., "Sodium D2 resonance radiation in single-pass sum-frequency generation with actively mode-locked Nd:YAG lasers," *Opt. Lett.* **32**, 1965-1967 (2007).
11. C. A. Denman, P. D. Hillman, G. T. Moore, J. M. Telle, J. E. Preston, J. D. Drummond, and R. Q. Fugate, "Realization of a 50-watt facility-class sodium guidestar pump laser," *Proc. SPIE* **5707**, 46-49 (2005).
12. S. H. Huang, Y. Feng, A. Shirakawa, and K. Ueda, "Generation of 10.5 W, 1178 nm laser based on phosphosilicate Raman fibre laser," *Jpn. J. Appl. Phys. Part 2* **42**, L1439-L1441 (2003).
13. A. B. Rulkov, A. A. Ferin, S. V. Popov, J. R. Taylor, I. Rozdobreev, L. Bigot, and G. Bouwmans, "Narrow-line, 1178nm CW bismuth-doped fibre laser with 6.4W output for direct frequency doubling," *Opt. Express* **15**, 5473-5476 (2007).
14. D. Georgiev, V. P. Gapontsev, A. G. Dronov, M. Y. Vyatkin, A. B. Rulkov, S. V. Popov, and J. R. Taylor, "Watts-level frequency doubling of a narrow line linearly polarized Raman fiber laser to 589 nm," *Opt. Express* **13**, 6772-6776 (2005).

15. T. P. Rutten, P. J. Veitch, C. d'Orgeville, and J. Munch, "Injection mode-locked guide star laser concept and design verification experiments," *Opt. Express* **15**, 2369-2374 (2007).
16. Y. Furukawa, S. A. Markgraf, M. Sato, H. Yoshida, T. Sasaki, H. Fujita, T. Yamanaka, and S. Nakai, "Investigation of the bulk laser damage of lithium triborate crystals," *Appl. Phys. Lett.* **65**, 1480-1482 (1994).
17. V. Z. Kolev, M. W. Duering, and B. Luther-Davies "Compact high-power optical source for resonant infrared pulsed laser ablation and deposition of polymer materials," *Opt. Express* **14**, 12302-12309 (2006).
18. http://www.tbwp.com/Sites/S_Products/PicosecondProducts_HP/Fuego.htm
19. <http://www.ilt.fraunhofer.de/eng/100994.html>
20. B. Luther-Davies, V. Z. Kolev, M. J. Lederer, N. R. Madsen, A. V. Rode, J. Giesekus, K. M. Du, M. Duering, "Table-top 50-W laser system for ultra-fast laser ablation," *Appl. Phys.-A, Materials Science and Processing* **79**, 1051-1059 (2004).
21. <http://www.as-photonics.com/SNLO>

1. Introduction

In 1953 the astronomer Horace Babcock proposed the concept of adaptive optics as a method for improving the resolution of astronomical telescopes by correcting distortions introduced by the atmosphere [1]. Now, over fifty years later, adaptive optical systems have finally become practical due to advances in laser, optical and electronic technologies [2,3]. An essential component of a modern adaptive optics telescope is the 589nm laser source needed to create an artificial guide star (laser guide star or LGS) by exciting resonance fluorescence from the mesospheric sodium layer 85-95km above the earth's surface. A number of 589nm sources have been demonstrated including early systems based on dye lasers [4]; sources based on sum frequency generation of the 1064nm and 1319nm lines of Nd:YAG [5,6,7,8,9,10,11]; and fibre lasers [12,13,14]. However, there remains scope for alternative schemes that offer simplicity, reliability, versatile pulse formats, power scaling and rapid tuneability to meet emerging needs, particularly of extremely large telescopes [15].

In this paper we describe proof-of-concept experiments leading to the generation of several watts of quasi-continuous 589nm emission from an optical parametric amplifier (OPA) pumped by a passively mode-locked Nd:YVO₄ MOPA (Master Oscillator Power Amplifier) system. A significant advantage of our approach is that it comprises a linear optical chain that could be assembled from commercially available hardware and does not require fast switching electronics or active cavity stabilization. The heart of the system is the pump laser that can be scaled to deliver powers of several hundred Watts or kilowatts at 1064nm using technology similar to that employed in the 50W, 1064nm laser used in these experiments. Other features of our system are that the output wavelength can be rapidly tuned on and off the sodium resonance line (at rates up to ≈ 1 kHz in our case) by simply controlling the frequency of a low power CW beam that seeds the parametric amplifier. It can operate with an arbitrary pulse train format (single pulse; continuous pulse train; pulse bursts; frequency modulated pulse train, etc). Linewidths at 589nm of around 3GHz should be achievable and are determined by the transform limit of the output pulse envelope. In the current experiments the minimum 589nm linewidth was limited by the use of shorter than optimum (92ps) 1064nm pump laser pulses and estimated to be ≈ 13 GHz.

2. Experimental approach

A parametric amplifier uses a second order nonlinear optical interaction to convert photons from a fixed pump frequency, ω_p , to signal and idler frequencies ω_s , ω_i respectively, such that $\omega_p = \omega_s + \omega_i$. When phase matching (momentum conservation) is satisfied, energy flows from the pump to signal and idler beams inducing a small signal gain, G , in the nonlinear crystal which can be written:

$$G = 1 + \text{Sinh}^2(GL) \text{ where } G = 4\pi d_{\text{eff}} \sqrt{\frac{I}{2\epsilon_0 n_p n_s n_i c \lambda_s \lambda_i}} \quad (1)$$

here L is the crystal length; $n_{p,s,i}$ are the refractive indices at pump, signal and idler wavelengths respectively; and $\lambda_{s,i}$ are the signal and idler wavelengths. For nonlinear crystals

even with small values of d_{eff} such as Lithium Triborate (LBO, $d_{eff} \approx 0.8 \text{ pm/V}$), the small signal gain can be very large ($>10^6$) at intensities well below the material damage. Such high gain is commonly employed in optical parametric generators (OPGs) where amplification of parametric fluorescence (noise) can result in significant pump depletion even in a single pass of the crystal. However in this instance the emission is relatively broadband since the gain bandwidth is large. This issue is overcome in an optical parametric amplifier where a narrowband CW seed beam at either the signal or idler frequency is injected at a power substantially exceeding that of the parametric fluorescence. This seed beam is amplified and can lead to strong pump depletion. The important point is that now the linewidth of the output at the seed wavelength is determined only by the Fourier transform of the envelope of the output pulse and that is determined by the time-dependent gain. If the pump pulse is transform-limited, then the output pulses in both the signal and idler beams are also transform-limited. As we will show later, the high gain required from the parametric amplifiers typically results in the output pulse duration being about half that of the pump. In the context of the laser guide star, we aim for a linewidth covering the full manifold of the Na D₂ lines $\approx 3 \text{ GHz}$ wide, and this requires a transform-limited Gaussian pulse with a duration $\approx 146 \text{ ps}$. Typically, therefore, the OPA would need to be pumped with a pulse around $\approx 300 \text{ ps}$ in duration.

There is a wide range of possible schemes for generating 589nm from an OPA. In this instance we restricted ourselves to a technologically robust route based on a Neodymium pump laser that offers the best opportunity for power scaling to the kW range (at 1064nm) if required. In addition, it has been shown that transform-limited pulses 200-300ps long can be generated via active or passive mode-locking using Nd:YAG or Nd:YVO₄ by adding an intracavity etalon to reduce the lasing bandwidth. Since optical parametric amplification requires rather high laser intensities (few $\times 10^9 \text{ W/cm}^2$), we chose to use Lithium Triborate (LBO) as the nonlinear optical crystal because of its well-established resistance to laser damage. For ns pulses, the bulk damage threshold for LBO is reported to be $>40 \text{ J/cm}^2$ [16]. LBO also offers the advantage of temperature-tuneable non-critical phase matching for all the interactions used in this work. A final requirement is the ready availability of a narrowband tuneable seed laser with power in the 10-100mW range. Thus, in order to generate 589nm light we chose the following scheme, shown in Fig. 1.

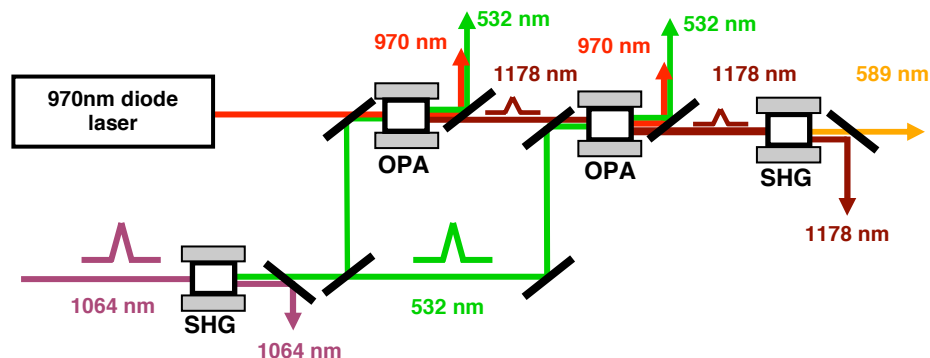


Fig. 1. Schematic of the system used to generate 589nm light using a two stage OPA pumped by 1064nm mode-locked Nd:YVO₄ MOPA laser.

The pump laser at 1064nm was first frequency doubled to 532nm. This 532nm beam was then used to pump a two-stage OPA comprising pre- and power amplifiers. The pre-amplifier was seeded with the narrow linewidth tuneable CW semiconductor diode laser at $\approx 970 \text{ nm}$ and generated amplified signal and idler pulses at 970nm and 1178nm respectively. The crystals were placed in ovens in order to set the required temperatures for phase matching. The required crystal temperatures were 143.7C for the SHG of 1064nm, 148C for the two OPA stages and 40.7C for the SHG of 1178nm. Whilst seeding at 1178nm would have been preferable (relaxing the need to ensure the pump pulses were transform-limited), diode lasers

are not currently available at this wavelength. The 1178nm idler output was amplified in the second (power amplifier) stage before being frequency doubled to create the required 598nm beam.

Whilst this requires three separate steps of nonlinear frequency conversion (SHG – OPA – SHG) each step can be efficient provided high enough pulse power is available from the laser. For example, the conversion efficiency for SHG of ≈ 15 ps 1064nm pulses from our mode-locked Nd:YVO₄ laser is more than 83% at intensities ≈ 1.5 GW/cm² using a 20mm long LBO crystal. Therefore, to achieve efficient conversion high pulse powers (>1 MW) will be required which allows GW/cm² intensities to be achieved in a beam whose confocal parameter is large compared with the typical crystal length – a few cm. The corresponding pulse energy will therefore be in the 300 μ J range. Thus, since adequate SHG efficiencies can be obtained, the critical parameter becomes the conversion efficiency of the OPA taking the inevitable losses to the signal wave into account. As we have reported earlier [17], the achievable conversion efficiency (i.e. the pump depletion) for a typical two-stage OPA is ≈ 50 -55% yielding the best overall efficiency from pump (532nm) to idler (1178nm) of ≈ 23 % or from 1064nm to 589nm of ≈ 15 %.

Using this last value implies that, for example, a 100W class laser producing ≈ 300 ps pulses at a repetition rate of about 300kHz is required to generate 15W of yellow light with ≈ 3 GHz linewidth. Recently lasers with close to this specification have been developed for industrial applications such as micro-machining. For example *Time-Bandwidth Products (TBP)* recently released the 50W *Fuego* system [18], whilst a combination of a *TBP Duetto* and an *Innoslab* amplifier [19] (*Fraunhofer Institut fuer Lasertechnik - ILT*) should be capable of exceeding the average power requirements by more than a factor of 2. As a consequence the pump laser can be regarded as available commercially.

For our experiments, however, we used a custom MOPA system based around an extended resonator SESAM mode-locked Nd:YVO₄ laser oscillator operating at 1.5MHz [20] with an *Innoslab* amplifier from *ILT* [19]. This laser was optimized to produce an average output power of 50W at 1064nm in pulses 15ps in duration at 1.5MHz and could be frequency doubled in a 20mm long LBO crystal to produce >40 W at 532nm in pulses 13.9ps long. By inserting an etalon with 40% reflectivity mirrors into the oscillator cavity the output pulse could be stretched to 92ps at 40W power at 1064nm and 27W at 532nm. Because of the higher than desired repetition rate of this laser and lower than required average power most OPA tests to assess conversion efficiency and beam quality were carried out using 13.9ps pulses which allowed similar beam intensities and average powers to those that would be encountered in the guide star configuration. Experiments with the longer 90ps pulses were used to demonstrate that the OPA output pulses were transform-limited.

The seed laser was a *Toptica Photonics DL100* grating stabilized tuneable semiconductor laser with a linewidth of <1 MHz; mode-hop free tuning range of ≈ 20 GHz; and output power ≈ 220 mW. The beam from this laser was spatially filtered by passing it through a short length of single mode optical fibre incorporating a polarization controller and focused to a spot $\approx 43\mu$ m in diameter in the pre-amplifier crystal leaving about 90mW available to seed the OPA.

The output of the pump laser was split into two beams using a polarizer and half wave plate and around 4W at 532nm was delivered to the pre-amplifier and the remaining 36W to the power amplifier. Two-lens telescopes were used to set pump beam intensities in all nonlinear frequency conversion stages. The idler output from the first stage was isolated using dichroic mirrors and directed to the power amplifier crystal. A delay line, realized with a retro-reflector on a micrometer stage, ensured time synchronization of the second stage pump pulses with the idler pulses generated by the pre-amplifier. The final OPA output was focused into a LBO frequency doubler to produce the 589nm output beam.

3. OPA performance

3.1 Pre-amplifier

Previously [17] we reported the performance of an OPA for generating tuneable mid infrared light and found that a two-stage OPA is the minimum required to obtain conversion efficiency (from pump to (signal + idler) – equivalent to the level of pump depletion) exceeding 50%. The pre-amplifier stage operates at very high small signal gain and amplifies the injected CW signal beam to form a train of output pulses at signal and idler wavelengths. The overall efficiency of this first stage is limited by reconversion to about 40% above which the output beam quality starts to deteriorate [17]. Because of the high gain the pre-amplifier crystal is also subjected to the highest fluence and hence is the stage most susceptible to laser damage. The output from the pre-amplifier stage is fed to a relatively low gain power amplifier that typically achieves a conversion efficiency of about 55%.

From these previous studies it was evident that the characteristics of the output pulse are determined primarily by the high gain pre-amplifier stage. In particular the duration of the generated pulses affect both the achievable conversion efficiency in the power amplifier stage and ultimately the linewidth of the emission. We, therefore, used the 2D-mix-LP model of the SNLO code [21] to study pulse shortening (the ratio of pulse duration of the amplified seed to the pump pulse at the OPA output) and pump depletion in the pre-amplifier. The model neglected group velocity effects which are insignificant for pulses longer than a few ps. The results are shown in Figs. 2, 3 and 4.

Figure 2(a) shows the measured and predicted pump depletion as a function of peak laser intensity whilst Fig. 2(b) shows pulse shortening as a function of pump depletion.

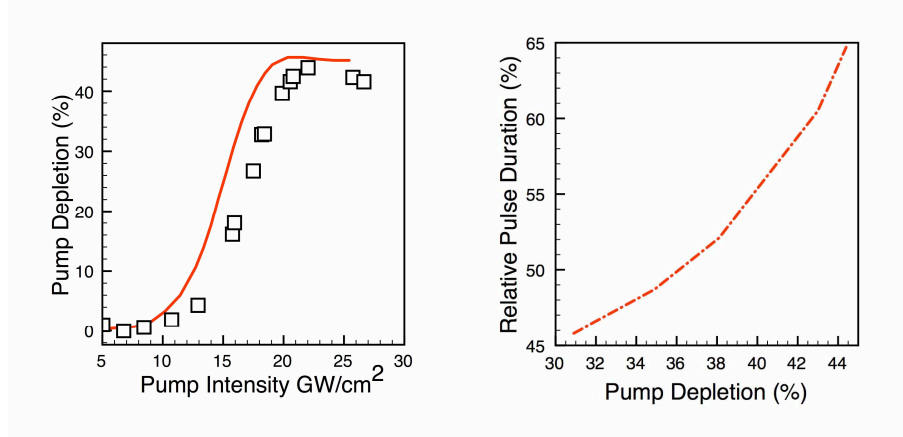


Fig. 2. (a). (LHS): Calculated (line) and measured (squares) pump depletion as a function of input intensity for the pre-amplifier stage; Fig. 2(b), (RHS): Calculated pulse shortening (output pulse duration at seed wavelength/pump pulse duration) as a function of pump depletion.

The maximum depletion of about 45% occurred at a peak intensity of 22GW/cm² above which back-conversion starts to clamp the conversion efficiency. The experimental data are in good agreement with the simulations with the small discrepancy attributable to the slightly less than perfect pump beam quality ($M^2=1.1, 1.3$ in vertical and horizontal planes respectively). Previously we reported that the output beam quality in the signal and idler deteriorated with the onset of back-conversion [17]. It is evident from Fig. 2(b) that back conversion has a beneficial effect, namely it lengthens the output pulse which can both reduce the pulse bandwidth and improve temporal overlap with the pump pulses in the power amplifier. Good signal and idler beam quality ($M^2<1.3$) is maintained at pump depletion of 40% (pulse shortening of 55%). However, a useful increase in the pulse duration (65% pulse shortening) can be achieved at the expense of beam quality if the pump depletion is pushed to its

maximum value around 45%. In further calculations, however, we assumed the operating point was chosen to achieve 55% pulse shortening.

3.2 Power amplifier

In the power amplifier stage the idler emitted from the pre-amplifier interacts with the residual pump. The interacting beams are large enough for beam divergence to be neglected in the simulations. In this situation, the conversion efficiency depends on the ratio of the pulse durations, $\tau_{\text{seed}}/\tau_{\text{p}}$ and beam diameters $d_{\text{seed}}/d_{\text{p}}$, of the seed and pump as well as the powers (intensities) in the two beams. We consider the conditions that optimise pump depletion in the power amplifier as well as how the system performance changes if one or several power amplifier stages are used.

As mentioned above, we fixed the operating point of the pre-amplifier to achieve 40% pump depletion and $\tau_{\text{seed}}/\tau_{\text{p}} = 0.55$. The predicted performance of a power amplifier stage in such conditions is shown in Fig. 3(a) using a 20mm long LBO crystal. Each curve represents different seed intensity. For every seed power there is an optimum value of the pump intensity at which the best conversion efficiency is obtained. As the seed intensity (power) is reduced, larger gains are required and this reduces the best conversion efficiency because of back conversion as in the case of the pre-amplifier. In Fig. 3(a) the ratio of $d_{\text{seed}}/d_{\text{p}}$ was chosen to be 1.8. This was identified as the optimal beam ratio by plotting a series of curves showing the peak conversion points such as those in Fig. 3(a) for different values of $d_{\text{seed}}/d_{\text{p}}$ and resulted in Fig. 3(b). This shows that a beam ratio is 1.8 achieves the highest conversion across a range of power ratios ($P_{\text{p}}/P_{\text{s}}$) from a few to a few hundred. For a power amplifier with $P_{\text{p}}/P_{\text{s}}$ of 10 the best conversion efficiency is $\approx 55\%$. Clearly the exact choice of beam size is determined by available laser power in the second stage.

The shape of the curves in Fig. 3(b) suggests that higher efficiency can be obtained from several power amplifier stages in tandem. For example, if a large signal gain of x100 is required, two x10 stages will provide a higher efficiency than a single stage with a gain of x100 (assuming no additional losses are incurred). We have analysed the achievable efficiency for conversion of a 1064nm pump to 1178nm idler beam by employing one, two or three OPA stages using as a parameter the fraction of the pump power directed to the final stage. The results are shown in Fig. 4. Clearly for a two stage system 70-80% of the available pump should be used in the power amplifier yielding an overall conversion efficiency of 22%. However, by using three or four stages the efficiency can increase somewhat to 26%.

Whilst this improvement is modest, it may well be worthwhile in systems operating with extreme pump powers especially where a single power amplifier would need to operate at high gain ($\gg 10$).

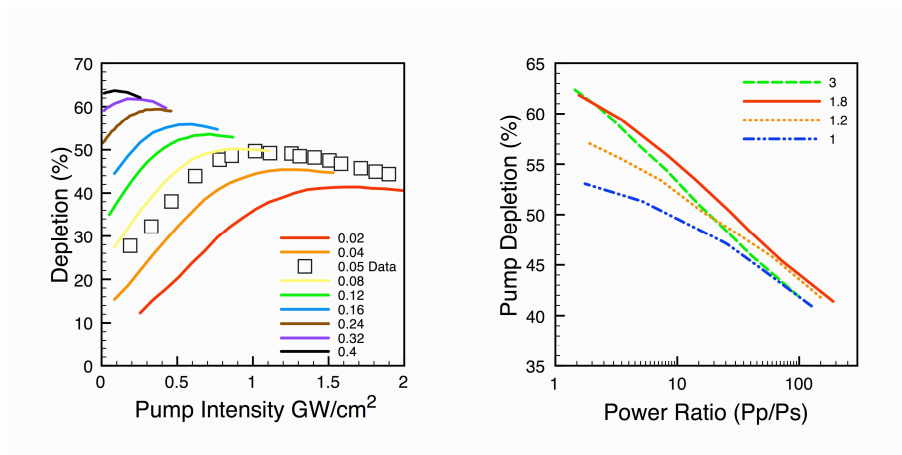


Fig. 3. (a). (LHS): Pump depletion achievable in the power amplifier stage as a function of pump intensity for different seed intensities (GW/cm²). In these calculations the ratio of the seed beam to pump beam diameter was set at 1.8 and τ_i/τ_p was assumed to be 0.55 (from Fig. 2(b)). Experimental data obtained using a seed intensity of 0.05GW/cm² is plotted for comparison with the results of simulations. Figure 3(b), (RHS): Pump depletion is plotted as a function of the ratio of the pump power to seed power in the power amplifier stage for four different values of the ratio d_{seed}/d_p .

Finally we note that these estimates should represent relatively conservative values of achievable conversion efficiency. For example an improvement can be expected if the seed pulse is lengthened by driving the pre-amplifier further into saturation, provided this does not lead to deterioration in output beam quality. Furthermore, because the power amplifiers are themselves strongly saturated, their output pulse is longer than their input pulse. Thus in a system with two or more power amplifiers, better conversion efficiency should be achieved than shown in Figs. 3 and 4 where the input pulse was assumed to be 55% of the pump pulse duration.

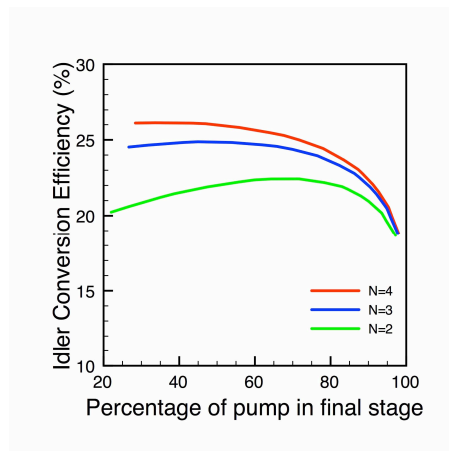


Fig. 4. Variation of maximum achievable conversion efficiency to the idler for 2, 3, and 4 OPA stages using the fraction of the total pump power used in the final stage as a parameter.

4. Experimental results

The performance of the pre-amplifier has already been presented in Fig. 2 in terms of conversion efficiency and showed good agreement with the modelling. Since the total available power at 532nm was 40W, we chose to use 4W in the pre-amplifier leaving a

maximum of 36W for a single power amplifier. The seed power at 1178nm produced by the pre-amplifier was $\approx 720\text{mW}$ at 40% pump depletion. According to Fig. 3(b), using $d_{\text{seed}}/d_p=1.8$ then it should be possible to obtain $\approx 55\%$ pump depletion from 7.2W of pump power ($P_p/P_s=10$). We used seed and pump spot sizes of $d_{\text{seed}}=570\mu\text{m}$ and $d_p=375\mu\text{m}$ respectively. The pump depletion was measured as a function of the pump power in these conditions and the results are plotted in Fig. 3(a). Good agreement with the modelling results was obtained and the peak efficiency was close to the predicted value at 51%. Using the full power available in the second stage resulted in a lower conversion of $\approx 46\%$ as expected since $P_p/P_s \approx 50$ (see Fig. 3(b)). The experimental data obtained from the power amplifier stage were in overall excellent agreement with the predictions of the model.

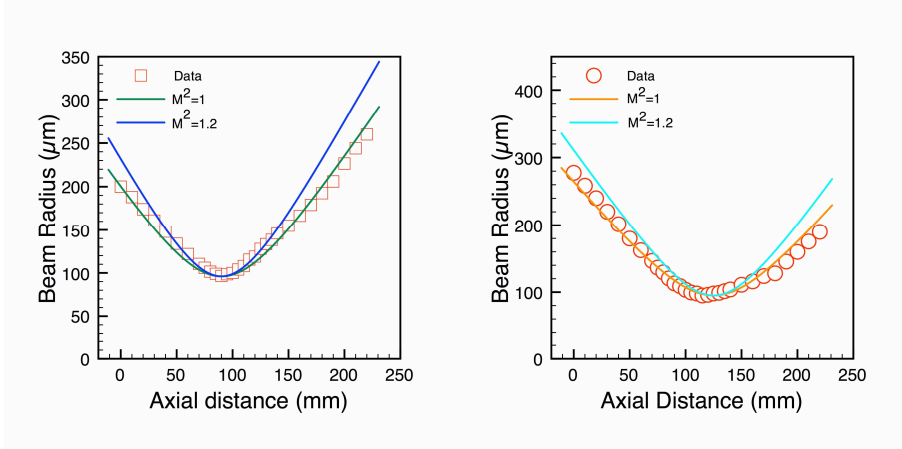


Fig. 5. Beam radius as a function of axial distance around focus compared with calculated values of M^2 . LHS: horizontal plane; RHS: vertical plane.

Feeding the maximum pump power to the power amplifier stage resulted in $\approx 7\text{W}$ being generated at 1178nm at the output. This was frequency doubled using a 20mm long LBO crystal to produce 5.5W at 589nm. Since high beam quality is essential for the LGS emission, the output beam quality at 589nm was determined from analysis of the M^2 value as show in Fig. 5. Values of $M^2_{x,y} < 1.2$ were obtained confirming that the beam quality from the OPA was excellent.

These results so far were obtained using short 13.9ps duration pulses from the pump laser which, as indicated earlier, led to fluences close to those that would be encountered in the optimised guide star configuration. However such short pulses result in significantly larger spectral bandwidth than desired. The output spectrum (FWHM at 1178nm) was measured using an Agilent optical spectrum analyser and found to be 65GHz, which is consistent with the production of transform-limited pulses 7-8ps in duration. However to determine whether transform-limited output pulses could be obtained with longer pulses, we inserted an etalon, 40% reflectivity, into the laser oscillator which stretched the output pulse duration (at 1064nm) to $\approx 92\text{ps}$ (determined both from autocorrelation and using an Agilent *Infinium* sampling oscilloscope and New Focus 1444 InGaAs detector). Pulses longer than 92ps could not be generated from our passively mode-locked extended cavity oscillator most likely because a fast, high modulation SESAM was needed to obtain stable mode-locking, and this caused the cavity losses to rise rapidly and the oscillator power to drop as an etalon with a narrower pass band was added. Using the same frequency doubling arrangement (optimised for 15ps pulses) we obtained a conversion efficiency of $\approx 71\%$ and $\approx 32\text{W}$ at 532nm in a pulse 78ps in duration. Because of the lower peak power in these longer pulses we only used the pre-amplifier for tests generating up to 4W at 1178nm which was converted to 3W at 589nm.

Measurements of the output spectrum were again performed using the Agilent OSA whilst the pulse duration at 1178nm was measured with both an autocorrelator and fast photodiode.

After correcting for the resolution bandwidth of the OSA (0.01nm), the linewidth of the output at 1178nm was found to be 11.4GHz at 43% pump depletion. The output pulse duration was measured to be 42ps yielding a time-bandwidth product of 0.48 – close to the expected value for a Gaussian pulse – and representing 54% of the input pulse duration (at 532nm) in agreement with the predictions of Fig. 2(b). Thus, we concluded that the output pulse was both transform-limited and had undergone the predicted degree of pulse shortening in the pre-amplifier. Simulations of the SHG process with SNLO indicated that at high SHG conversion efficiency, as used in these experiments, the generated pulses are $\approx 10\%$ shorter than the pump pulses. This results in a $\approx 10\%$ increase in bandwidth at 589nm relative to the 1178nm bandwidth, making the 589nm line width $\approx 13\text{GHz}$.

A special feature of this 589nm source is that the output frequency can be directly controlled by tuning the CW seed laser. Thus the output could be easily locked to the Na D_2 line using the Pound-Drever-Hall technique, or alternatively the frequency can be scanned on and off the Na D_2 resonance line if required. We believe this latter feature may provide a significant advantage for LGS applications since, for example, it can allow the sensor in the wavefront detector to discriminate against Rayleigh scattered light. To demonstrate this we tuned the output wavelength of the DL100 laser by $\approx 20\text{GHz}$ on and off the Na D_2 line and imaged the fluorescence emission and scattered light from a cell containing Na vapour at 200C. Only a few mW of 589nm power was used in this experiment. By subtracting the off-resonance from the on-resonance images the scattered light signal could be effectively removed (Fig. 7). Since the DL100 laser can be tuned at rates around 5GHz/ms, it should be possible to subtract consecutive images from the sensor in the Shack-Hartman wavefront sensor at kHz rates. It would be difficult to obtain such fast tuning using other 589nm sources.

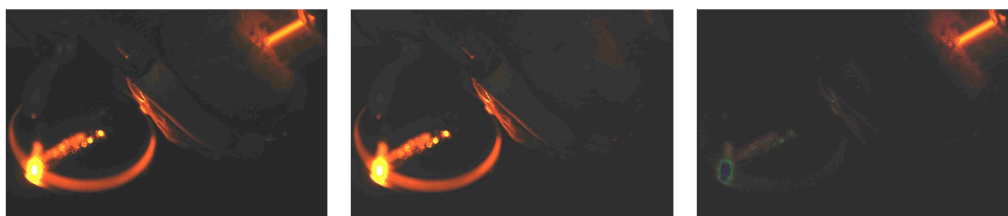


Fig. 7. LHS: image of fluorescence from a Na vapour cell (streak in the upper right) and scattered light from a mirror at the cell output (lower left) with the laser tuned to the Na D_2 resonance; Centre: laser tuned off resonance; RHS: difference between first two images demonstrating discrimination against scattered light.

5. Conclusion

We have described the operation of a multi-stage optical parametric amplifier seeded by a tuneable CW semiconductor diode laser and pumped by a passively mode-locked Nd laser. The particular feature of this scheme is that it provides a straightforward way of generating transform-limited pulses in diffraction-limited beams at 589nm for LGS applications using commercial laser hardware. Whilst many routes for generating 589nm emission could be envisaged, in these proof-of-concept experiments we chose to use the most straightforward and robust route where we generated 589nm emission using nonlinear optical processes (SHG, OPA) only in damage resistant Lithium Triborate crystals pumped by a high average power Nd:YVO₄ laser. Using this scheme the best conversion efficiency (1064nm-589nm) we achieved was 12% although it should be possible to increase this to about 15% with further optimisation. There is room to increase the overall conversion efficiency by improving the dichroic coatings of the optical components, increasing the seed power in the pre-amplifier and by optimizing the pump power ratio between pre- and power amplifier. Our modelling shows that ideally 30% of the available pump power should be used in the pre-amplifier to optimize overall efficiency (Fig. 4), while we used around 10%. With increased seed power, the pumping of the pre-amplifier at higher average power levels would become feasible.

Because the technology our laser is based upon has been demonstrated to be scalable to average power >1000W at 1064nm, we believe our scheme provides a straightforward route to creating LGS with powers exceeding 100W.

The OPA-based LGS offers possible additional advantages over other schemes. Firstly it provides broadband emission covering the full width of the Na D₂ lines reducing the impact of saturation and secondly it allows rapid (kHz) electronically controlled tuning of the output frequency on and off the resonance with the possible advantage of reducing the impact of Rayleigh scattered light on the adaptive optics system. Since the OPA is a linear chain, its performance is insensitive to the pulse format allowing the generation of single pulses, bursts of pulses or quasi-continuous pulse trains.

Acknowledgments

The authors gratefully acknowledge the support of the Australian Research Council through its Linkage Grants and Federation Fellowship program for this research.